



# RICH DETECTOR FOR THE EIC'S FORWARD REGION PARTICLE IDENTIFICATION

An Updated EIC R&D Proposal

June 27, 2014

Fernando Barbosa<sup>e</sup>, William Brooks<sup>i</sup>, Marco Contalbrigo<sup>d</sup>,  
Amaresh Datta<sup>h</sup>, Marcel Demarteau<sup>a</sup>, J. Matthew Durham<sup>f</sup>,  
Douglas Fields<sup>h</sup>, Xiaochun He<sup>c</sup>, Hubert van Hecke<sup>f</sup>(co-PI),  
Jin Huang<sup>b</sup>, Ming Liu<sup>f</sup>, Jack McKisson<sup>e</sup>,  
Yi Qiang<sup>e,\*</sup>(co-PI, contact), Patrizia Rossi<sup>e</sup>,  
Murad Sarsour<sup>c</sup>, Robert Wagner<sup>a</sup>, Wenze Xi<sup>e</sup>,  
Liang Xue<sup>c</sup>, Zhiwen Zhao<sup>g,e</sup>, Carl Zorn<sup>e</sup>

*a. Argonne National Lab, Argonne, IL 60439*

*b. Brookhaven National Lab, Riverhead, NY 11901*

*c. Georgia State University, Atlanta, GA 30303*

*d. INFN, Sezione di Ferrara, 44100 Ferrara, Italy*

*e. Jefferson Lab, Newport News, VA 23606*

*f. Los Alamos National Lab, Los Alamos, NM 87545*

*g. Old Dominion University, Norfolk, VA 23529*

*h. The University of New Mexico, Albuquerque, NM 87131*

*i. Universidad Tecnica Federico Santa Maria, Valparaiso, Chile*

\* Email: [yqiang@jlab.org](mailto:yqiang@jlab.org)

## Table of Contents

Abstract .....	2
1. Motivation .....	3
2. Technology Overview .....	6
2.1. Choice of Radiators.....	6
2.2. Dual-Radiator Concept .....	10
2.3. Modular Concept .....	12
2.4. LAPPD Readout.....	13
2.5. GEM-Based Readout .....	16
3. Goals and R&D Activities.....	18
3.1. Detector Simulation .....	18
3.2. Study of MCP-based LAPPD .....	20
3.2.1. Year 1 – Characterization .....	20
3.2.2. Year 2 – Improvement.....	22
3.3. Development of Photosensitive GEM Readout .....	23
3.3.1. Year 1 – Initial development .....	23
3.3.2. Year 2 – Combined Tests .....	24
3.4. Selection of Aerogel Tiles .....	24
4. Budget .....	26
5. Further Work .....	29
6. Summary .....	29
Bibliography .....	30

# **RICH DETECTOR FOR THE EIC'S FORWARD REGION PARTICLE IDENTIFICATION**

June 27, 2014

## **Abstract**

An R&D program is proposed to investigate the technology to be used for a Ring Imaging Cherenkov (RICH) detector for the hadron particle identification in the forward region of the future Electron-Ion Collider (EIC). Both the dual-radiator RICH option and a modular RICH concept will be investigated and the associated special optics design will be carried out. In particular, a newly developed Large-Area Picoseconds Photo-Detector (LAPPD) using renovated Micro-Channel Plate (MCP) technology will be carefully evaluated as the readout of the RICH detector. If feasible, the excellent timing resolution provided by this new readout will greatly improve the PID capability of the RICH detector. In parallel, a GEM-based readout option will be investigated as well. The main goal of this project is to determine the best detector technology and to provide a conceptual design of the RICH detector for the EIC. This is an updated version of the original proposal RD 2013-4 [1].

## 1. Motivation

The future Electron-Ion Collider (EIC) [2] will target on several hot physics topics, such as the nucleon tomography and quark orbital angular momentum accessible through the study of the generalized parton distributions (GPDs) and the transverse-momentum dependent parton distribution functions (TMDs), the quark hadronization in nuclear medium and the hadron spectroscopy. A dedicated EIC detector is currently under development and its conceptual schematic is shown in Figure 1. It is imperative to develop new detector technologies for carrying out the crucial physics measurements.

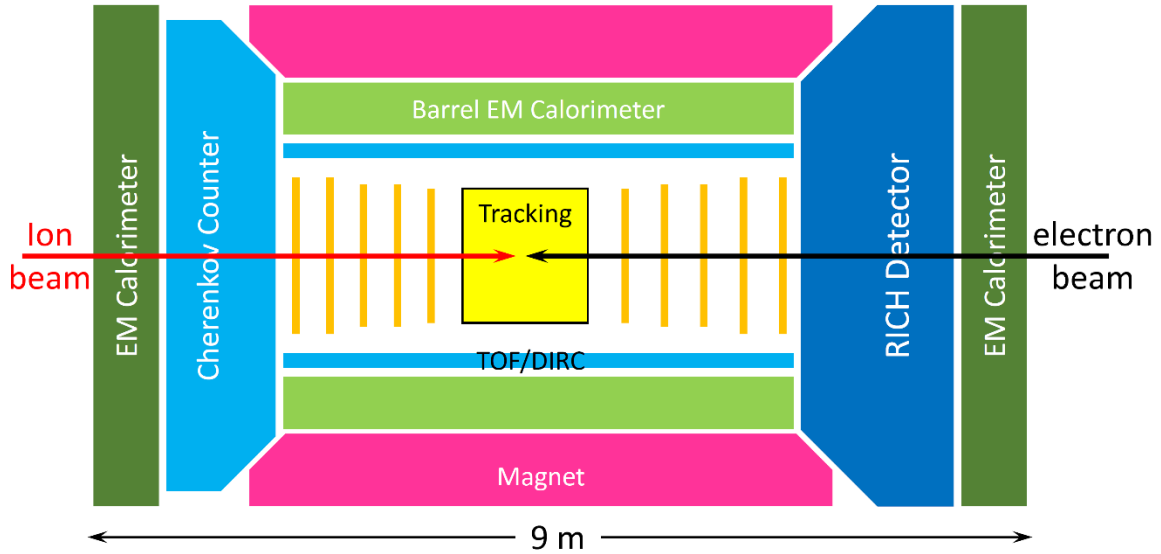


Figure 1. A schematic view of an EIC detector conceptual design.

In this proposal, we are mainly concerned with hadron identification in the forward and backward region (rapidity  $|y| > 1$ ). Using the semi-inclusive DIS (SIDIS) as an example, SIDIS is a powerful tool for disentangling the distributions of different quark and anti-quark flavors. It is also the golden channel to study the TMDs and it further allows us to investigate the full three-dimensional dynamics of the nucleon. While the detection of pions provides information mainly regarding light quarks, kaon identification is particularly important for studying sea quark distributions. As shown in Figure 2, the momentum of SIDIS pions in the forward and backward region typically ranges from less than 1 GeV to about 15 GeV. In Figure 3 we can also see that pions greatly outnumber kaons over the whole kinematic region. In most of the momentum range the kaon yield is only about 10 – 15% of the pion yield. Therefore a  $4\text{-}\sigma$   $K/\pi$  separation is desirable for clean kaon identification.

## RICH Detector for the EIC's Forward Region PID

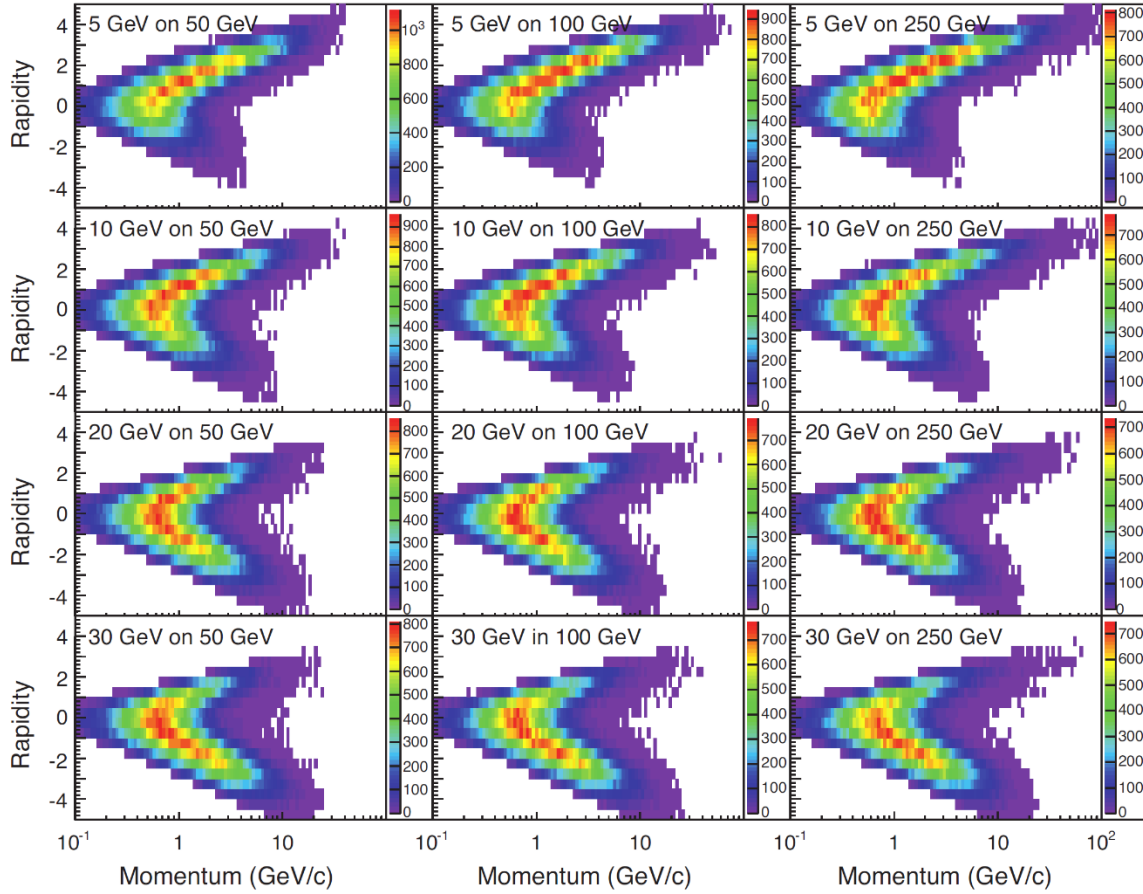


Figure 2. Momentum vs. rapidity in the laboratory frame for pions from semi-inclusive deep inelastic scattering (SIDIS) reactions [1]. The following cuts have been applied:  $Q^2 > 1 \text{ GeV}^2$ ,  $0.01 < y < 0.95$  and  $z > 0.1$ .

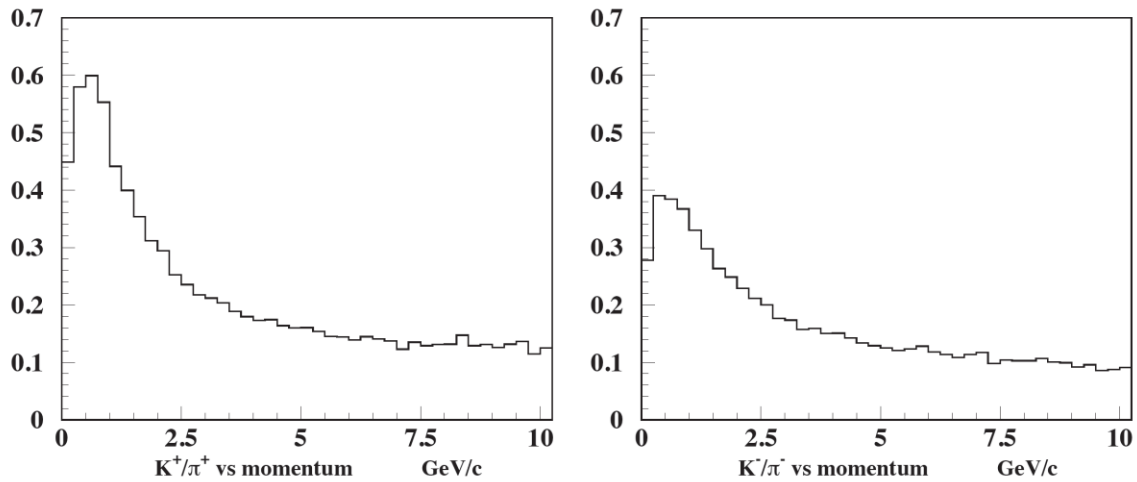


Figure 3. Kaon/pion ratio vs. momentum in the laboratory system from SIDIS events in the forward region (rapidity  $y > 1$  and for a  $10 \times 100 \text{ GeV}$  configuration).

## RICH Detector for the EIC's Forward Region PID

In order to cover such a large momentum range a combination of various particle identification (PID) technologies is needed. In the low momentum range (0 – 3 GeV), PID can be achieved by a high resolution time-of-flight (TOF). For the higher momentum range (3 – 15 GeV), the most viable detector options are the Ring Imaging Cherenkov (RICH) detectors with dual radiators, or two RICH detectors with radiators of different refractive indices. Each radiator will provide unique sensitivities to different kinematic regions. As illustrated in Figure 4, an aerogel RICH detector would provide kaon identification for the intermediate  $x$  and  $Q^2$  region, and a gas radiator would provide unique coverage in the high  $x$  and  $Q^2$  region. In next section, we will discuss in more details about the choice of different radiators and readout options.

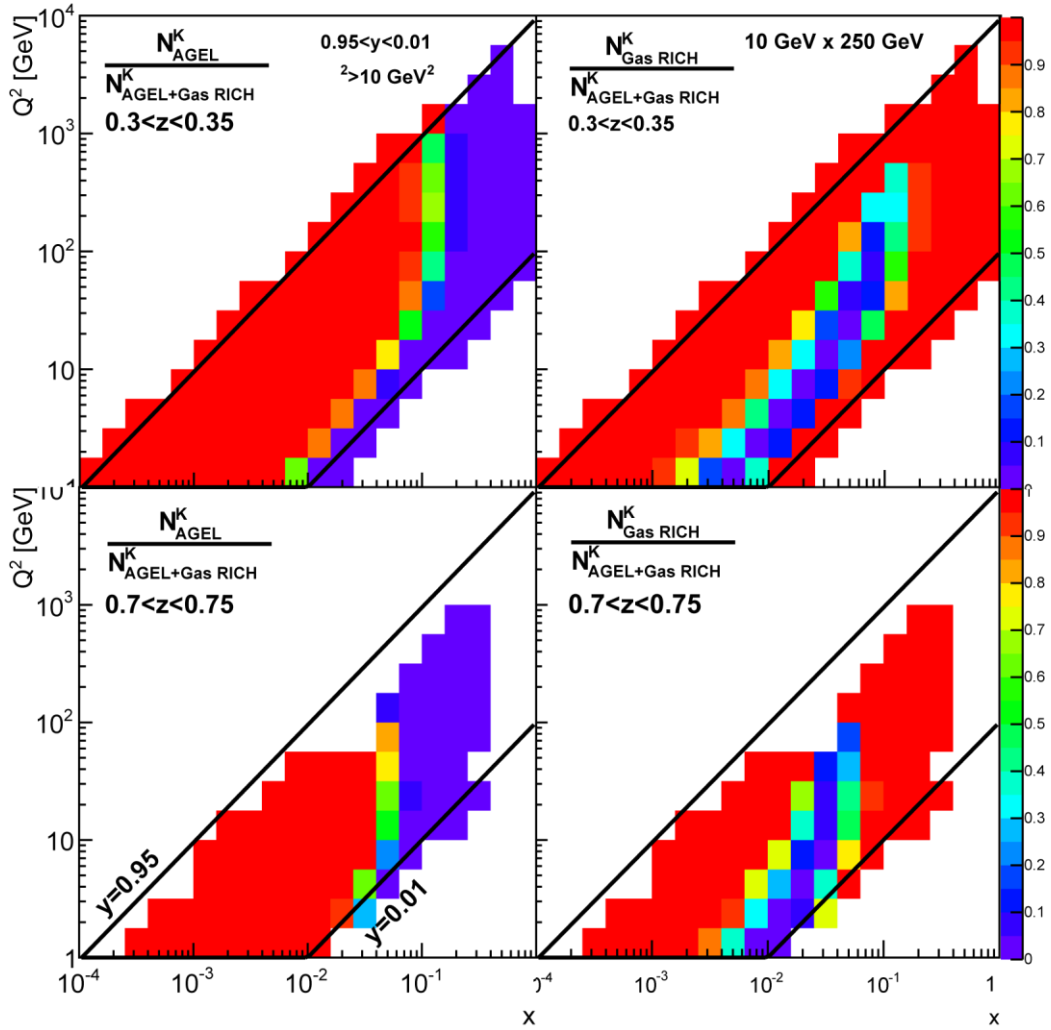


Figure 4. Yield ratios for SIDIS events with identified Kaons as function of  $x$  and  $Q^2$ , for an EIC detector with a barrel PID detector, a forward gas RICH and a forward aerogel RICH. Shown are the ratios when the forward gas RICH (left) or the forward aerogel RICH (right) are removed. Higher and lower  $z$ -ranges are shown in the top and bottom rows. This particular study is from the PHENIX collaboration [3] for a  $10 \times 250$  GeV beam configuration.

## 2. Technology Overview

### 2.1. Choice of Radiators

Table 1 List of properties of the commonly used Cherenkov radiators.

Material	Index	$N_0$ ( $\text{cm}^{-1}$ )	Max Angle (rad)	Threshold (GeV)		
				Pion	Kaon	Proton
N <sub>2</sub>	1.000298	0.06	0.024	5.53	20.27	40.26
CO <sub>2</sub>	1.000449	0.09	0.030	4.5	16.52	32.8
CF <sub>4</sub>	1.000482	0.1	0.031	4.35	15.94	31.66
Freon 12 (CCl <sub>2</sub> F <sub>2</sub> )	1.001073	0.21	0.046	2.91	10.68	21.21
C <sub>4</sub> F <sub>10</sub>	1.00137	0.27	0.052	2.58	9.45	18.77
Aerogel 1.01	1.01	1.18	0.141	0.95	3.49	6.93
Aerogel 1.02	1.02	2.33	0.198	0.67	2.46	4.89
Aerogel 1.05	1.05	5.58	0.310	0.42	1.55	3.07
Freon (C <sub>6</sub> F <sub>14</sub> )	1.2989	40.73	0.692	0.16	0.6	1.19
Fused Silica (SiO <sub>2</sub> )	1.473	53.91	0.825	0.12	0.46	0.91

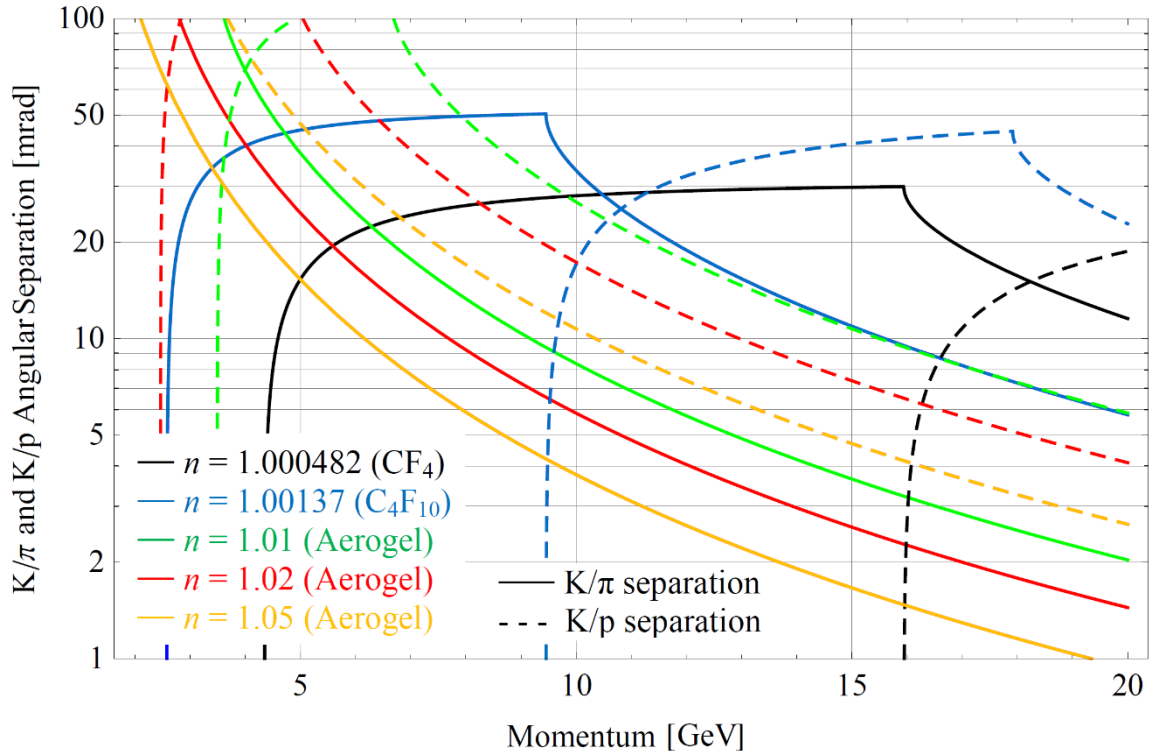


Figure 5. Angular difference of Cherenkov radiation produced by different charged particles.

## RICH Detector for the EIC's Forward Region PID

As shown in Table 1 and Figure 5, in order to cover the mid-momentum range (3 – 10 GeV), the refractive index of the radiator needs to be between 1.01 and 1.05. In this range, silica aerogel is the only proper material to use. Silica aerogel has been used for decades in threshold Cherenkov counters in high energy physics experiments, but more recently it has also been used as radiator material for RICH detectors in several particle physics experiments such as HERMES, LHCb, AMS, BELLE, etc. (See [4][5][6] and references therein). The optical properties of aerogel are the crucial parameters for the performances of RICH detectors. For instance, any angular dispersion of the emitted photons affects the precision of the Cherenkov angle measurements. In addition, a high transparency (Transmittance) and a proper refractive index ( $n$ ) are required in order to collect a sufficient number of photons for a reliable ring reconstruction. The measured transmittance  $T$  of an aerogel sample of thickness  $t$ , as function of the light wavelength  $\lambda$  is usually parameterized with the Hunt formula

$$T = Ae^{-Ct/\lambda^4}$$

which assumes that the absorption of the light, parameterized by  $A$ , is independent of the wavelength  $\lambda$  and that the Rayleigh scattering has a  $\lambda^{-4}$  dependence. The clarity coefficient  $C$  is proportional to the radiation scattered per unit of sample length, and is usually measured in  $\mu\text{m}^4/\text{cm}$ . Clarity is a measure of the quality of the sample - as  $C$  decreases more photons exit unscattered. Aerogel with a good optical quality therefore has values for  $A$  and  $C$  close to 1 and 0, respectively.

Absorption length ( $\Lambda_{\text{abs}}$ ) and scattering length ( $\Lambda_{\text{sc}}$ ) (in cm) are related to  $A$  and  $C$  through

$$\Lambda_{\text{abs}} = -t/\ln(A) \quad \text{and} \quad \Lambda_{\text{sc}} = \lambda^4/C$$

At present, aerogel tiles of large size and with good optical properties are produced by Novosibirsk group [7][8] in Russia. Samples of different refractive indices ( $n = 1.03, 1.04, 1.05$ ), thicknesses and sizes, produced in different periods, have been characterized by the INFN group by means of a spectrophotometer and tested in dedicated test beams (CERN, INFN-LNF). The INFN group is currently building a proximity focusing RICH for the CLAS12 [9] spectrometer of Hall B at Jefferson Lab. The group also tested several high-quality aerogel samples produced in Japan by Chiba University [10] for the BELLE-II experiment [11][12] and a few tiles from the US Aspen company [13].

In Figure 6, a comparison of the transmittance measured as a function of wavelength is presented for two Novosibirsk tiles (black and blue) and two Chiba tiles (red and pink) for nominal refractive index  $n = 1.05$  and thickness  $d = 2$  cm. As it can be seen clearly, the Novosibirsk and Chiba tiles have about the same transmittance and at 400 nm the measured transmittance of 2 cm tiles is of the order of  $\sim 65\%$ . However, the Novosibirsk tiles won the edge in scattering length, which is crucial for RICH application. A very good value of clarity better than  $0.0050 \mu\text{m}^4/\text{cm}$  has been extracted from the Novosibirsk samples. One thing worth mentioning is that the aerogel tiles produced by the Chiba group is hydrophobic while the Novosibirsk tiles are hydrophilic. The latter type requires

## RICH Detector for the EIC's Forward Region PID

a lot of care such as special handling and gas system to preserve its performance. In Figure 7, the performance of Aspen tiles with  $n = 1.01$  (blue) and  $n = 1.05$  (green, red and yellow) is compared with an  $n = 1.05$  Novosibirsk tile (black). The better optical quality of the Novosibirsk aerogel is clearly evident.

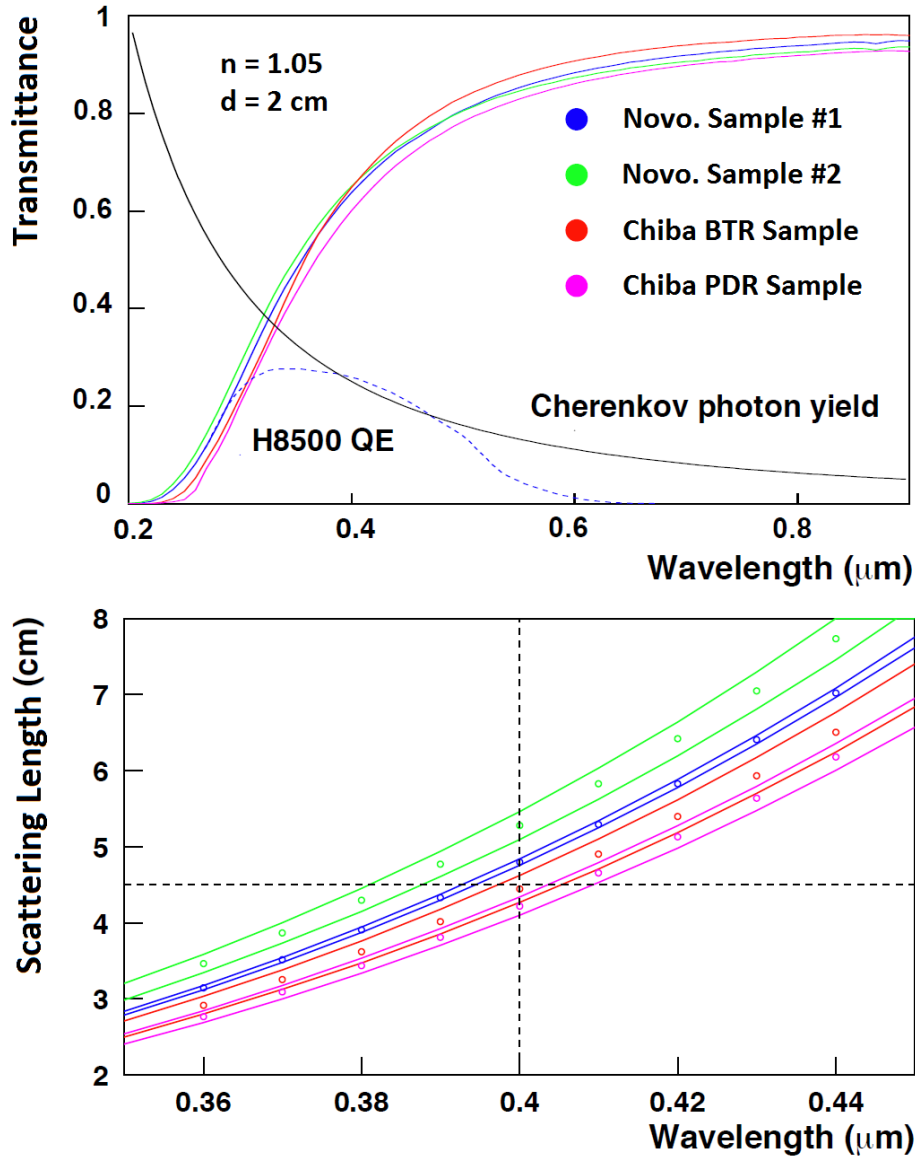


Figure 6. Comparison of the transmittance and scattering length measured as a function of the wavelength for two Novosibirsk tiles (black and blue) and two Chiba tiles (red and pink). All tiles have nominal refractive index  $n = 1.05$  and thickness  $d = 2$  cm. Five measurements were made on different positions along the aerogel surface, and the points show the average and the lines are the spread of the measured values. The typical quantum efficiency of Hamamatsu H8500 multi-anode PMT is shown as reference.

Over the past few years, significant improvement of aerogel's optical quality has been achieved. Both the Russian and Japanese groups have the capability and stable

## RICH Detector for the EIC's Forward Region PID

environment for R&D on optical parameters and mass production of aerogel tiles. Further improvements of production parameters in particular towards larger thickness and tile size could be necessary for the EIC RICH. Thus an R&D phase with these aerogel production companies is foreseen for this project.

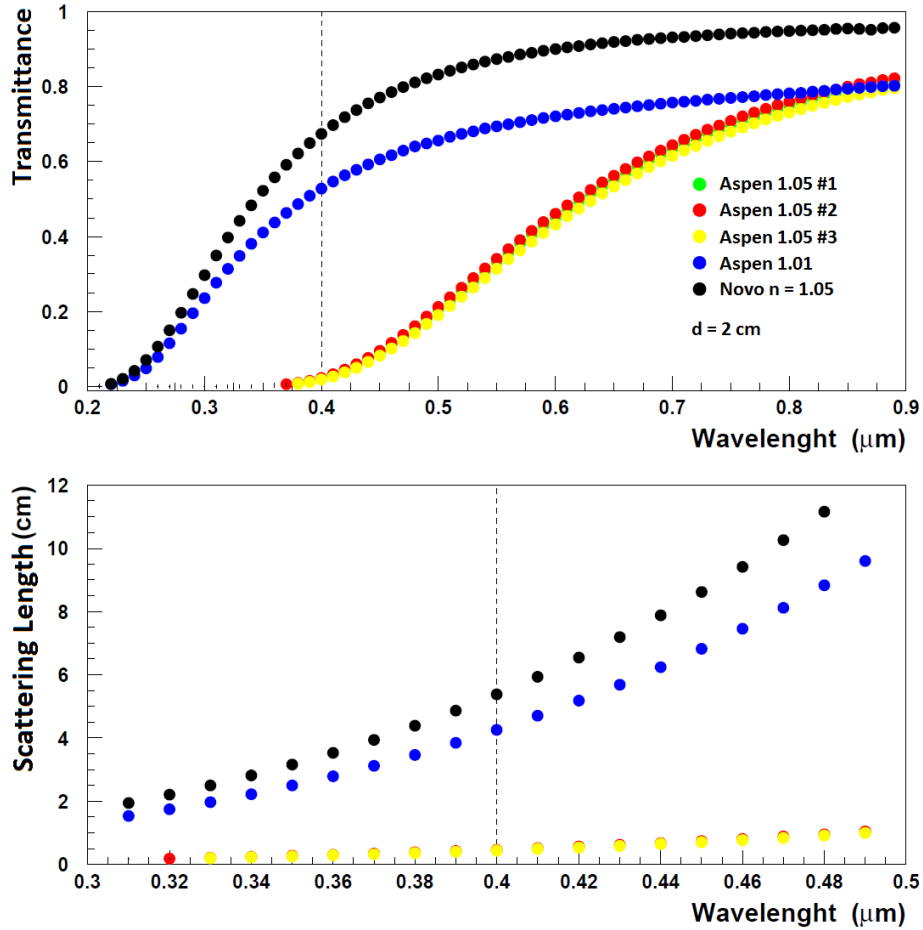
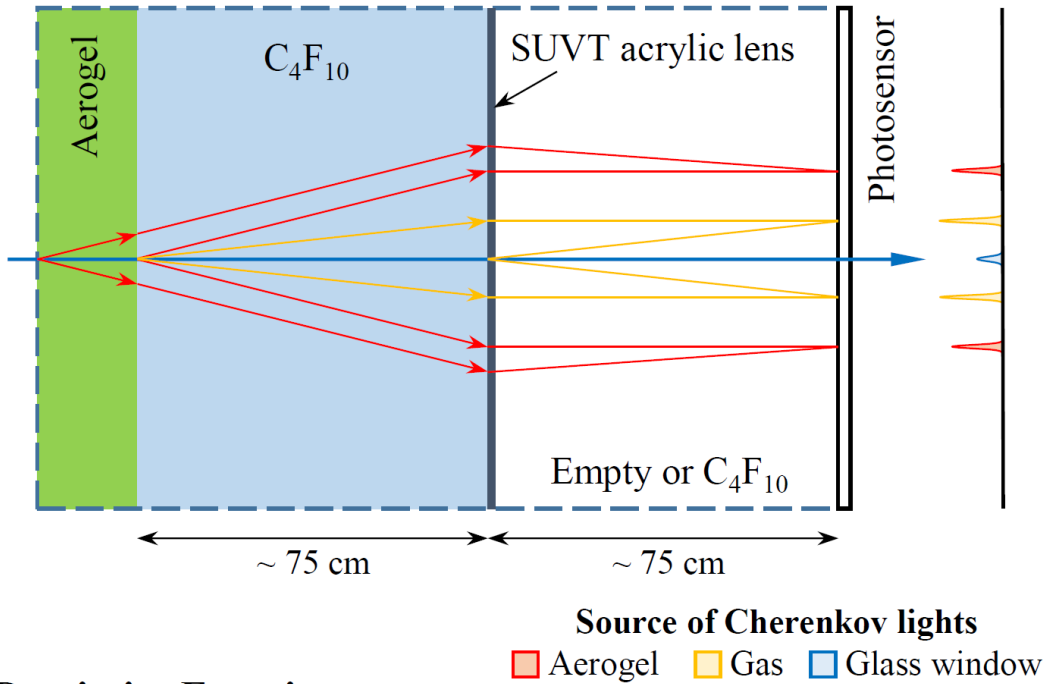


Figure 7. Transmittance and scattering length of the  $n = 1.01$  (blue) and  $n = 1.05$  (green, red and yellow) 2 cm Aspen tiles compared with an  $n = 1.05$  Novosibirsk tile (black).

For the high-momentum range (10 – 15 GeV), a gas radiator needs to be considered. Due to the low yield of Cherenkov light in gas, a large volume of gas is needed to produce enough photons. The refractive index of the gas determines how kaon will be identified in this momentum range. As shown in Figure 5,  $C_4F_{10}$  has a threshold low enough for kaon to produce Cherenkov lights, while  $CF_4$  can only serves as a veto counter for kaons with momentum less than 17 GeV.

## 2.2. Dual-Radiator Concept

### Focusing



### Proximity Focusing

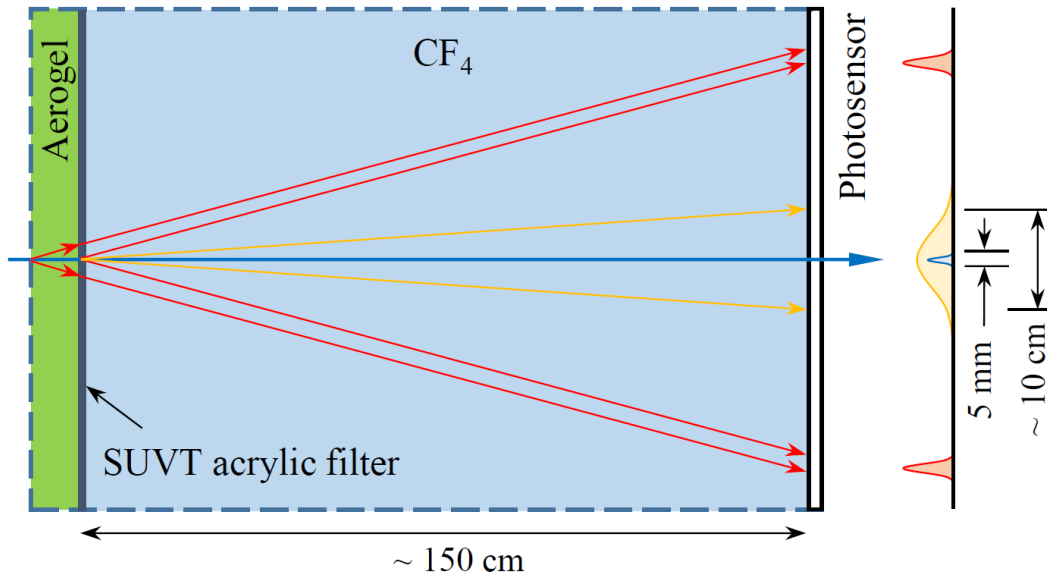


Figure 8. Concepts of the dual-radiator RICH detector for the EIC. Top: a concept with focusing using a Fresnel lens; Bottom: a concept using proximity focusing.

A dual-radiator RICH detector has the advantage of a more compact size and lower cost by using a shared readout, when compared with two separate Cherenkov detectors. Figure 8 shows two concepts of dual-radiator RICH detectors for the EIC. The length of both devices is chosen to be about 150 cm, given the space available in the MEIC design.

## RICH Detector for the EIC's Forward Region PID

The first concept shown on top is a focusing RICH detector. In this concept, an aerogel radiator is put in the front to cover the 3 – 10 GeV momentum range. Following the aerogel is a 75 cm long gas radiator volume containing  $C_4F_{10}$  to cover the 10 – 15 GeV range. The Cherenkov photons generated in each of the radiators are then focused by a Fresnel lens with a focal length of 75 cm. A super ultraviolet transmitting (SUVT) acrylic lens may be used to allow transmission of Cherenkov photons with wavelengths longer than 280 nm, as shown in Figure 9. The lens also serves as a filter to absorb UV lights which are strongly scattered by the aerogel. With about 10 – 20 photoelectrons per Cherenkov ring, the required position resolution of the readout is a few millimeters in order to reach  $4\text{-}\sigma$  kaon/pion separation. Furthermore, because of the spatial resolution of the readout device, the photosensors don't need to be placed at the focal plane of the lens, but can be moved closer to reduce the total length of the detector.

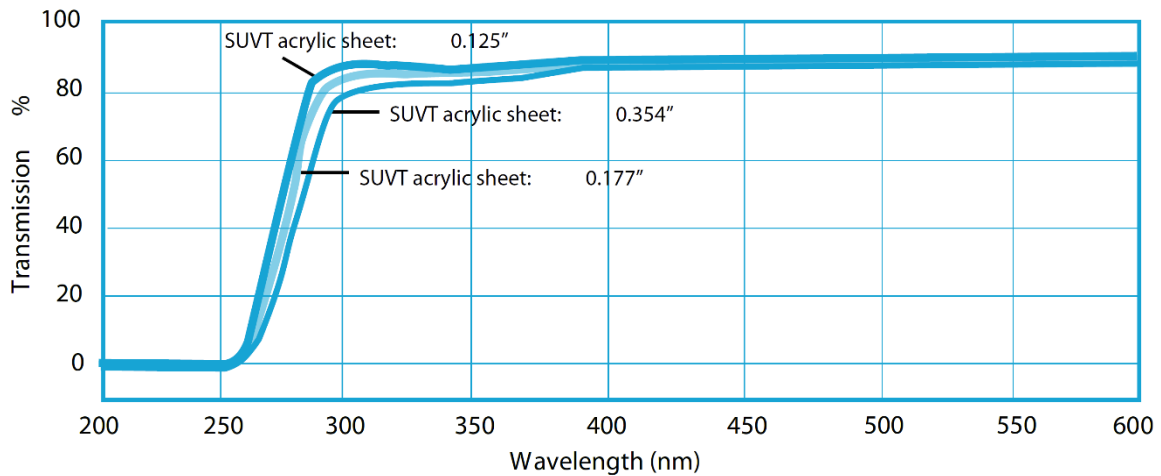


Figure 9. Transmittance of super ultraviolet transmitting (SUVT) acrylic sheet [14].

The second concept is a proximity focusing RICH detector. The first radiator is still aerogel. In order to achieve a reasonable angular reconstruction with proximity focusing, the thickness of the aerogel has to be limited to a few centimeters and the readout needs to be far away. Hence a 150-cm long volume is left between aerogel and readout. This volume will be filled with  $CF_4$  gas and serves as a threshold Cherenkov detector to veto pions up to 17 GeV. A layer of SUVT acrylic is added after the aerogel to suppress the scattered UV background. In the high momentum range (10 – 15 GeV), the separation of kaons and protons will still rely on aerogel. Although the proximity design seems much simpler in terms of optics design and mechanical construction, one big challenge will come from the Cherenkov radiation in the glass window of the readout sensors. Because of the photocathode coating, Cherenkov photons will exit the window and produce photoelectrons in the photocathode, instead of being trapped inside the window due to internal reflection. The hits generated by these photoelectrons will be concentric with the Cherenkov hits originated from  $CF_4$ . The coverage and amplitude of such a background signal depend on the window thickness. A 2 mm window typically generates about 10 photoelectrons with a spread of 5 mm. With a 2-dimensional readout, these signals from

glass window can be removed by applying geometric cuts. Nevertheless, thinner windows will clearly help suppress this kind of background.

Both concepts shown here are still in a very preliminary stage. More effort will definitely be needed in order to identify the best option with optimal optical design and an appropriate combination of radiators. These efforts are part of this proposed project.

### 2.3. Modular Concept

In parallel to the dual-radiator concept, we will develop a modular design for aerogel RICH detectors. In this design, we assume that a separate gas RICH detector would provide high momentum hadron ID (e.g. the gas-RICH under the support of current proposal RD-6 [15]). Meanwhile, we will focus on the hadron PID between  $p = 3 - 10$  GeV region using a single aerogel radiator.

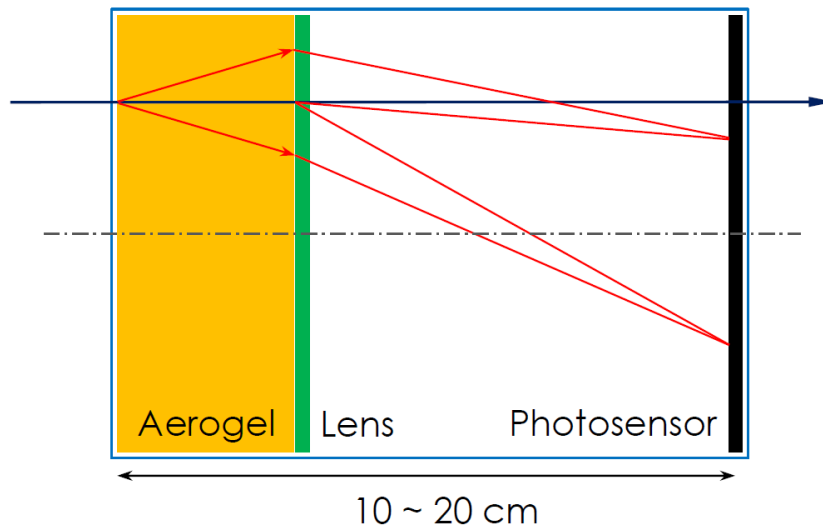


Figure 10. Diagram of a modular imaging aerogel detector, which consists of an aerogel radiator (orange), a Fresnel lens (green) and a photon detector (black). A module would be 10-20cm across.

In this scheme, a large detector would be constructed with smaller and independent units. A schematic of one unit is shown in Figure 10. Each unit would contain a Cherenkov radiator, in this case aerogel (orange), followed by an acrylic Fresnel lens (green), which focuses the Cherenkov photons onto a photon detector (black). In addition, the acrylic lens functions as a filter blocking scattered, low-wavelength photons. The scale of this unit would be determined by the size of the aerogel tiles used (assuming a single tile per unit), or by the size limitations of available Fresnel lenses or readout systems, but is expected to be of scale 10 – 20 cm. For particles that are incident parallel to the axis of the unit, Cherenkov rings would be centered in the unit's axis. The lens' focal length should be chosen such that the ring is smaller than the unit's diameter. Off-axis incident tracks result in rings offset from the center, but if the off-axis angular distribution is limited, the diameter of the sensitive area could be smaller than the size of

the unit. The spatial resolution of the photon detector will be determined by the requirement that kaons and pions be distinguished at the upper end of the momentum range. Since the ring size in the modular design is expected to be of order of a few cm, the pixel size will likely be small, less than 1 mm.

Full simulation of these units in the experimental environment will determine the parameters of this scheme, such as the necessary resolution of the photon detector, the focal length *etc.* When more than one charged particle traverses a given module, position and momentum information available from other detectors will be used in combination with the ring-hit distributions to determine the particle identities. Detailed algorithms will be developed based on full simulations.

## 2.4. LAPPD Readout

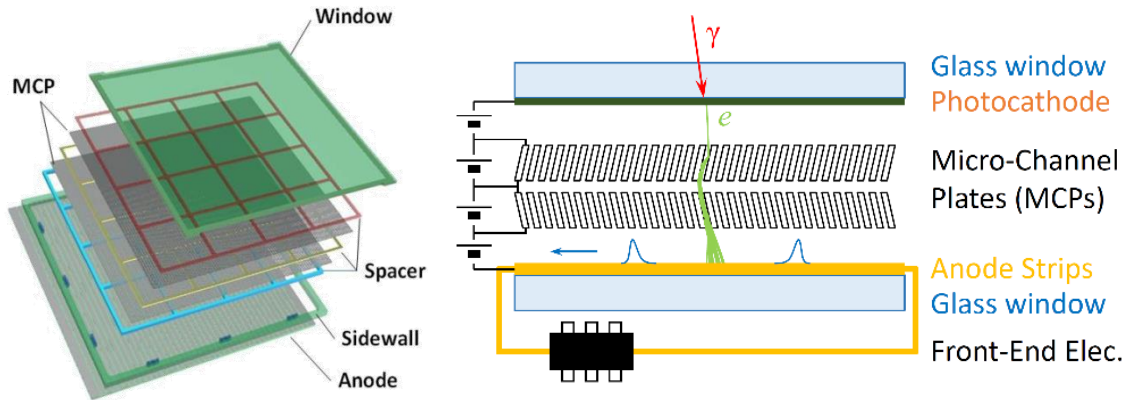


Figure 11. The Schematics of MCP-based LAPPD. Typical size is  $20 \times 20 \text{ cm}^2$ .

Starting in 2009, the development of a large-area picosecond-scale time resolution photo-detector has been carried out by the large-area picosecond photo-detector (LAPPD) collaboration [16]. The goal of their R&D program is to develop a family of large-area robust photodetectors using micro-channel plate (MCP) technology with excellent space and time resolution [17]. Furthermore the new devices should be relatively economical to produce in quantity. Figure 11 shows a schematic of such a photodetector. Photons are incident on a photocathode coated on the inner surface of the entrance window and the produced photoelectrons accelerate across a potential gap toward a pair of high-gain structures consisting of thin plates with high secondary electron emission (SEE) enhanced, micro-engineered pores. Voltages of roughly 1 kV are applied across each plate. Each electron entering a pore accelerates and strikes the pore walls, producing an avalanche of secondary electrons. The avalanche builds until the amplified pulse exits the bottom of the second MCP. This electrical signal is collected on an anode structure at the bottom, and passes through the vacuum assembly to front-end electronics, which digitize the signal.

## RICH Detector for the EIC's Forward Region PID

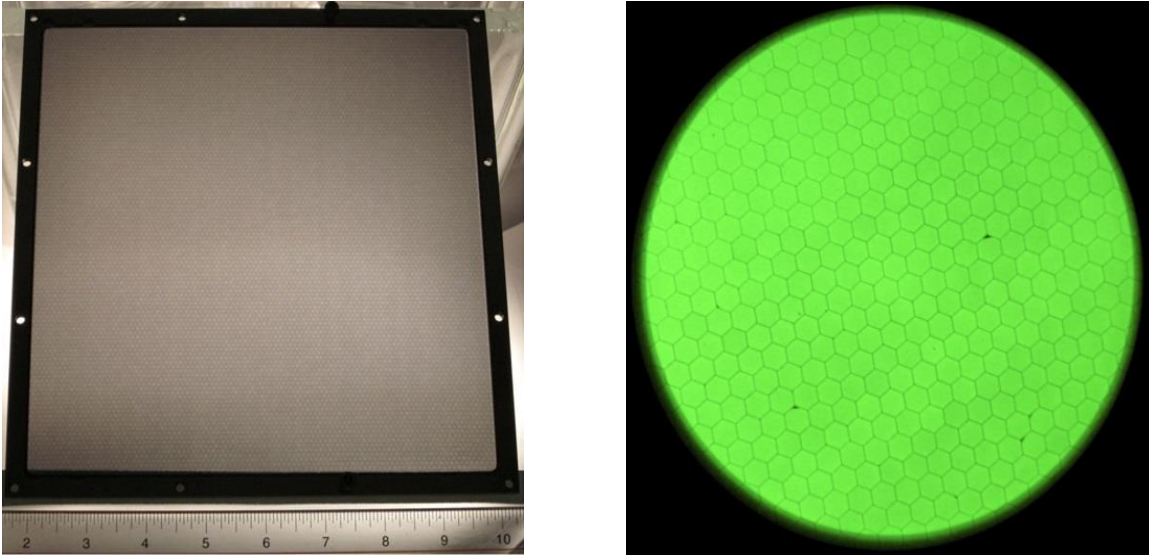


Figure 12. Left: photograph of a  $20 \times 20 \text{ cm}^2$  MCP made using ALD treatment of a borosilicate glass micro-capillary array.  $20 \text{ }\mu\text{m}$  pores,  $1.2 \text{ mm}$  thickness; Right: image for UV illumination onto an ALD coated borosilicate MCP with  $20 \text{ }\mu\text{m}$  pores,  $1.2 \text{ mm}$  thickness. The hexagonal multi-fiber packing structure is clearly visible.



Figure 13. The 3-tile anode, a total coverage of  $20 \times 60 \text{ cm}^2$ . The connections between anode strips on neighboring tiles have been made by soldering small strips of copper to the silver silk-screened strips on the glass [19].

To reach the goal, the LAPPD collaboration applied atomic layer deposition (ALD) on capillary glass channel substrates to produce MCPs [18] as shown in Figure 12, and has achieved better gain uniformity, much longer life-time and more robust performance than standard commercial MCPs made of lead glass but at much lower cost. Large area photocathodes have been coated on the glass windows using thermal evaporation with quantum efficiency (QE) over 25% at 350 nm wavelength. The anode readout uses strip transmission lines [19] sampled by front-end waveform sampling chips [20]. The position of a hit along individual strips will be calculated based on the time difference of the signals reaching the two ends. This design requires much fewer readout channel count while still maintaining a good spatial resolution  $< 5 \text{ mm}$ , which is comparable with other commonly used but more expensive pixelated photo detectors, such as Silicon

## RICH Detector for the EIC's Forward Region PID

Photomultipliers (SiPM) and Multi-anode Photomultiplier Tubes (MaPMT). Under low rate conditions, the readout of tiles can be chained as shown in Figure 13 to further reduce the number of channels. All these features make the LAPPD a very attractive economical candidate for the readout of a large area Cherenkov detector.

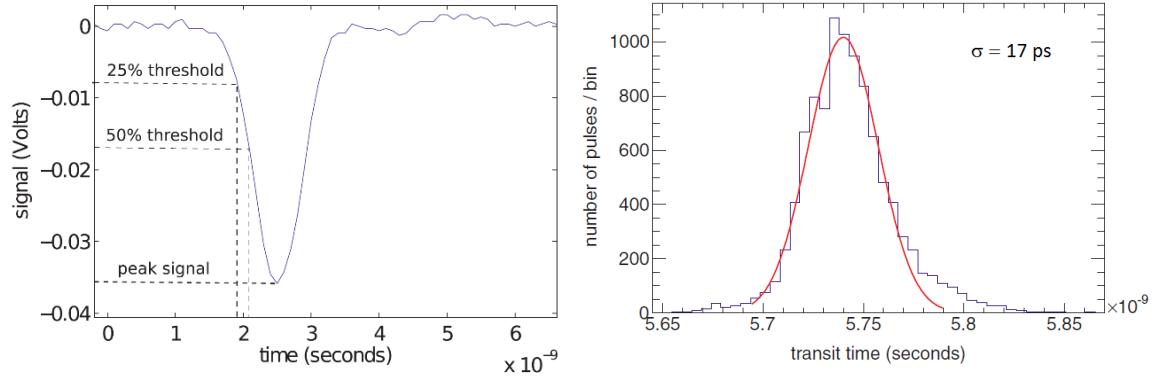


Figure 14. Left: an example of a MCP pulse showing the peak signal and the crossing time for a 50% and 25% constant fraction threshold. Right: measured time distribution of signals from a demountable LAPPD assembly using a focused 100-fs pulsed laser source [21].

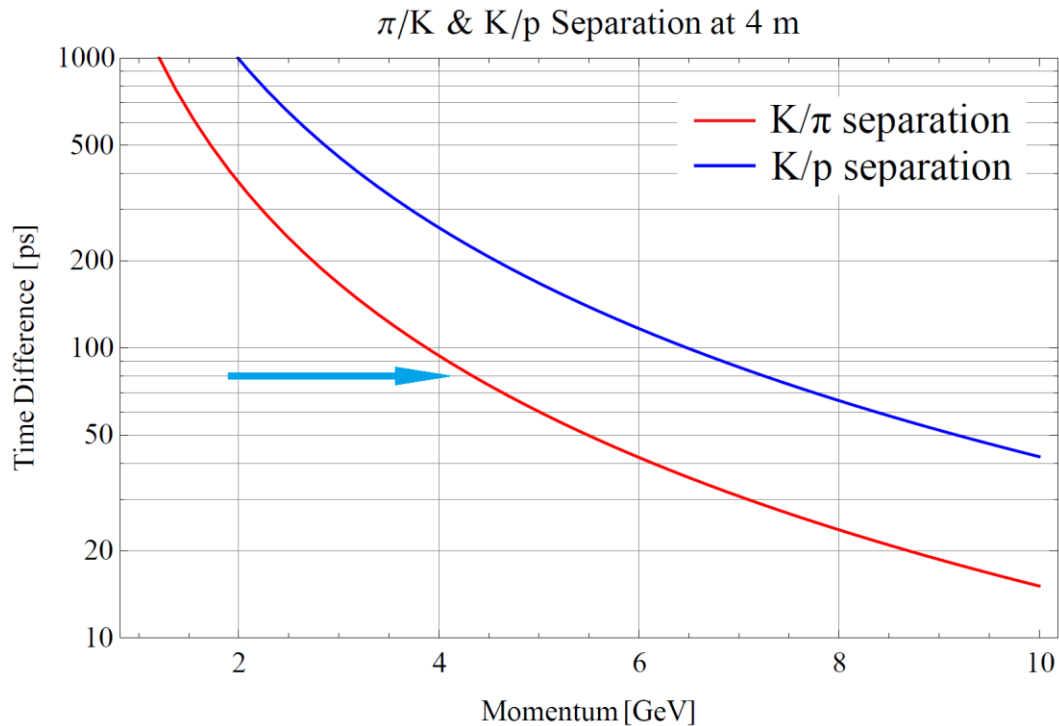


Figure 15. Difference in time-of-flight of kaon and pion and a path of 4 meters.

For initial testing, the collaboration assembled a  $20 \times 20$  cm<sup>2</sup> all-glass demountable prototype using an O-ring top window seal and an aluminum photocathode. This prototype has been operated for the past two years and demonstrated that exceptional time resolution can be achieved by this new device [21]. The absolute time resolution of a

single photon is about 44 ps and the uncertainty of the signal transition time in anode strips is only 17 ps<sup>1</sup>, as shown in Figure 14. With such good resolution, the LAPPD can also be used as an excellent time-of-flight (TOF) detector for identification of low momentum charged particles. One way is to use the photodetector's front glass window as a Cherenkov radiator to produce photons. Instead of being internally reflected, these photons will be absorbed by the photocathode coating and emit electrons. Assuming that on average 10 photon electrons are collected after a 2-mm thick window glass, the time resolution is expected to be better than 20 ps when convoluted with a beam's typical RF signal uncertainty. By looking at Figure 15, with a detection plane 4 meters away from the interaction point, the LAPPD can provide a  $4\sigma$  kaon/pion separation up to 4.2 GeV.

The LAPPD collaboration has assembled a  $20 \times 20$  cm<sup>2</sup> ceramic body prototype with  $QE > 25\%$  that successfully produced signals when excited with a UV laser inside the vacuum processing tank. Currently, the collaboration is focusing its effort on small form factor units with  $6 \times 6$  cm<sup>2</sup> active area MCPs which are more suitable for faster fabrication and prototyping. A vacuum transfer system at Argonne National Lab was put together and a few small detector units with aluminum and Bi-Alkali photocathodes have been successfully sealed in the system. At that time the heating available in the system was not sufficient to activate the non-evaporative getter (NEG) that will eventually be included in the device. This limits the useful lifetime of these first devices to approximately a week. The system is undergoing its final commissioning work and the first tubes to be made with the complete process are expected in late July, 2014. The first batch of fully functioning samples is expected to be available for user evaluation in the coming months.

## 2.5. GEM-Based Readout

GEMs with a reflective photocathode film deposited on the uppermost surface have recently emerged as an attractive photon detection technology [22], see Figure 16. Since the amplification structure is effectively decoupled from the charge collection plane, the geometry of the readout pattern can be optimized for the desired resolution with a minimal channel count. GEMs are available in various sizes from a range of foreign and domestic manufacturers. GEMs function well in magnetic fields. They have also been shown to operate in a variety of gases that are transparent in the wavelength range of interest, which minimizes Cherenkov photon losses.

In the wavelength range of interest for unscattered Cherenkov photons produced in aerogel,  $\sim 300 - 500$  nm, alkali crystals such as Sb-Cs-K have the necessary quantum efficiency (QE) to function as photocathodes as shown in Figure 17. Early studies by Breskin *et al.* [23] have shown a reasonable QE when deposited onto GEM foils. However, the effective QE is also strongly dependent on the choice of gas, which affects photoelectron scattering back into the photocathode. On the other hand, the group of III-

---

<sup>1</sup> The difference between these two uncertainties, 17 ps and 44 ps, can be attributed to the uncertainties of the photoelectric process in the photocathode, the drift of electrons in the gaps and the avalanche process in the pores.

## RICH Detector for the EIC's Forward Region PID

V semiconductor materials, such as GaAs, have relatively high quantum efficiencies in the wavelength range of interest to this project and are much more stable than bialkali photocathodes. Part of this research will grow and study both types of photocathodes and find the appropriate combination of the photocathode and working gas or mixture for the photosensitive GEM to detector visible lights.

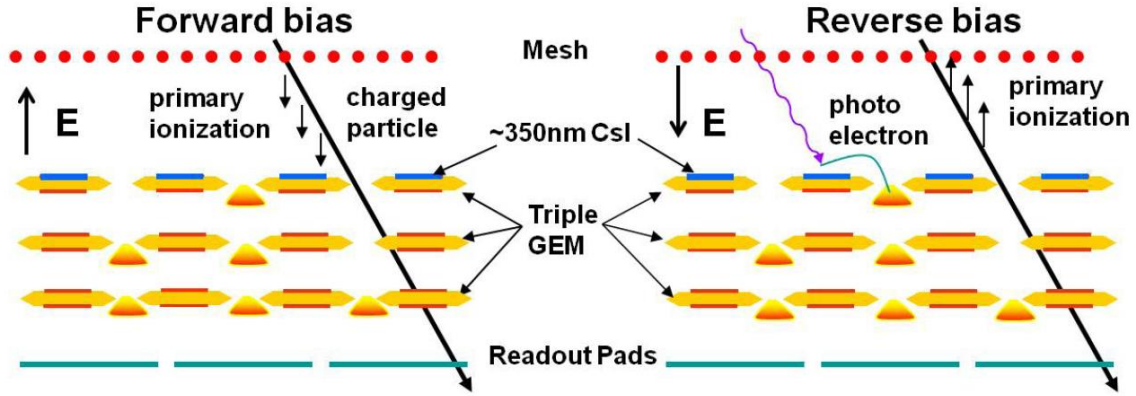


Figure 16. Triple GEM stack operated in the standard forward bias mode (left) and in the hadron-blind reverse bias mode (right) [22].

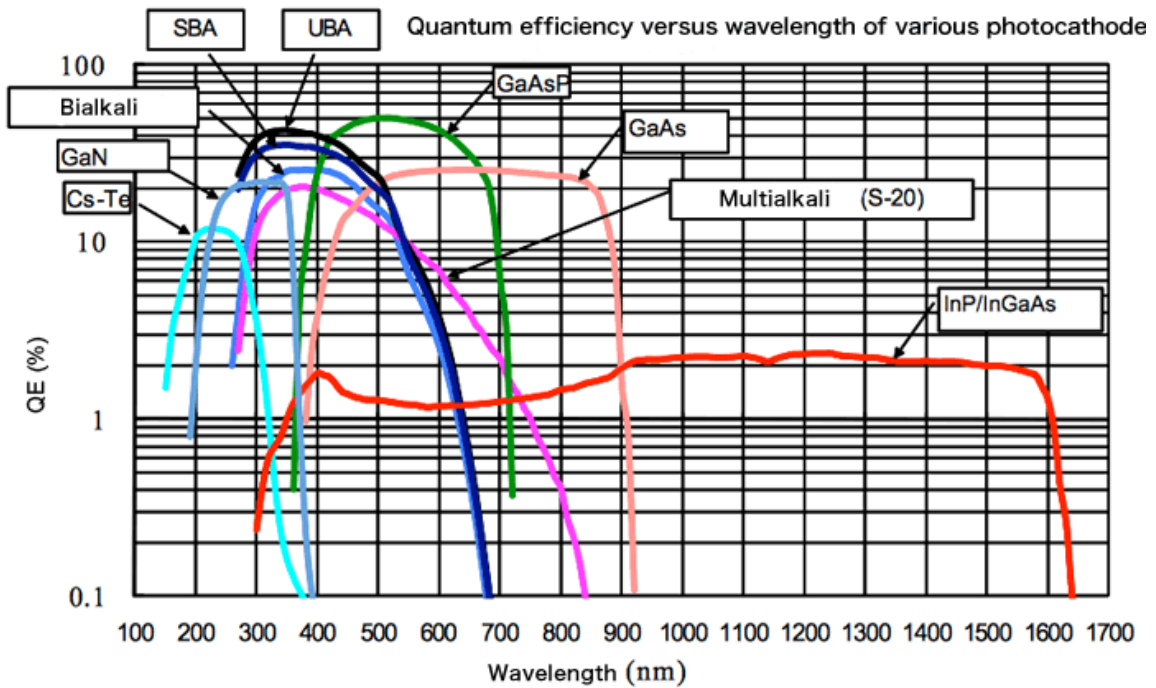


Figure 17. Comparison of quantum efficiency curves with various photocathode materials from Hamamatsu Photonics Corporation.

### 3. Goals and R&D Activities

The goal of the project is to determine the detector technology and to provide a conceptual design of the RICH detector in a course of two years.

We will carry out feasibility studies in various aspects toward a conceptual design:

- Detector simulation.
- Study of MCP-based LAPPD photodetector.
- Development of Photosensitive GEM photodetector.
- Selection of aerogel tiles.

Upon the completion of the project, with the chosen detector technology and the conceptual design, further work is anticipated for continuous development and producing prototypes of such RICH detectors for the EIC.

#### 3.1. Detector Simulation

The goal of the detector simulation is to obtain the requirements on various components of the RICH detector, to aid the development of the conceptual design and to justify its performance in a full EIC detector and beam environment. The major simulation studies are listed as follows:

- Implementation of the optical elements.
- Requirements on aerogel tile: refractive index, uniformity, flatness and clarity.
- Requirements on the photodetector: rate capability, sensitive wavelength, single photon detection efficiency, position resolution, field sensitivity and radiation tolerance.
- The effects of multiplicity and ambiguity with different readout/charge-collection segmentations - strip and pixels.
- Development of a preliminary ring reconstruction algorithm.
- Performance study of the RICH detector in a generic EIC detector model and in the full EIC collision environment.

An initial standalone Geant4 implementation of the modular concept has been constructed, as shown in Figure 18. A conceptual dual-radiator RICH detector was also created using a Geant3 framework as shown in Figure 19. In a next phase, both models will be imported into the larger simulation framework. The basic framework to be used is the GEMC [24] (GEant4 Monte-Carlo) based MEIC simulation [25] developed and maintained by Jefferson Lab. It serves as a C++ wrapper interface with Geant4. With this framework, the detector subsystems, geometry, material, field, and sensitive volumes are configured as external inputs to GEMC. The MEIC-GEMC has the capability of customizing the hit processing routine and output according to various detector requirements. In overall, these features allow us to simulate individual sub-detectors and the integrated detector system within the same framework and make it effortless to switch between them. With modularized design, the MEIC-GEMC framework can easily

## RICH Detector for the EIC's Forward Region PID

incorporate the proposed RICH detector into the simulation to study its performance and how it can work with other detector systems together to achieve the physics goals. Dr. Zhiwen Zhao, jointly hired by Old Dominion University and Jefferson Lab, is one of the authors and the current maintainer of the MEIC-GEMC software. He will provide guidance and support of the simulation. A JLab postdoc (25%), together with one postdoc (Dr. Liang Xue, 25%) and one student (50%) from Georgia State University will conduct the simulation work. The GSU group is playing a major role for studying the sPHENIX [28] calorimeter performance using Geant4 and has accumulated extensive knowledge of Geant4 simulation in general. Co-PI Yi Qiang from JLab and Dr. Jin Huang from BNL will coordinate the effort as they are both very experienced with designing large scale detector systems such as JLab's GlueX [26], SoLID [27] spectrometers, and BNL's sPHENIX [28] spectrometer and an EIC detector based on BaBar magnet at eRHIC [3].

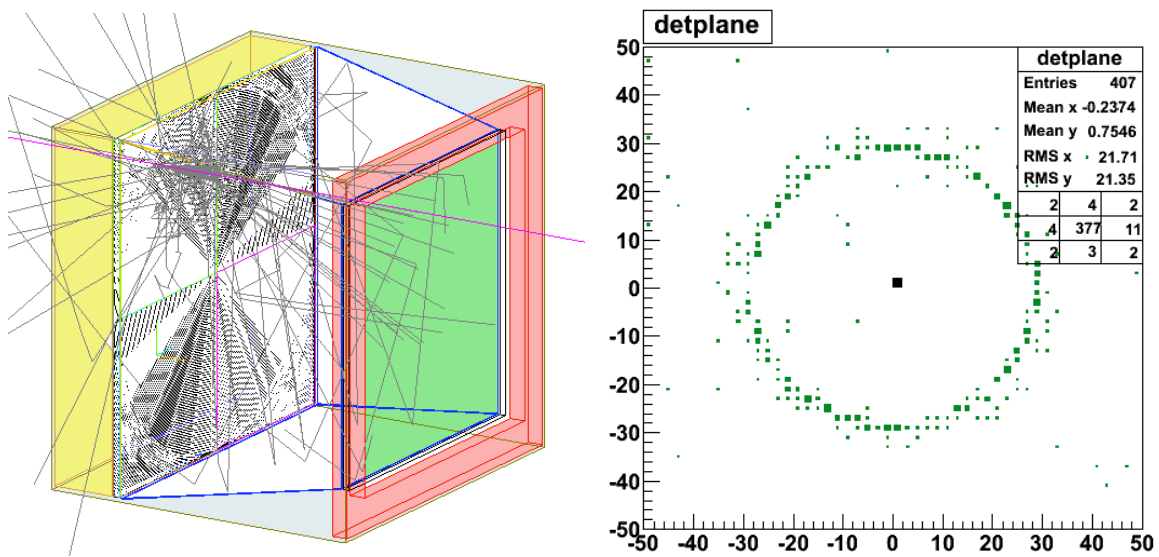


Figure 18. Implementation of a modular counter unit in Geant4. Left: visible are Aerogel (yellow), a Fresnel lens, flat mirrors (blue), photodetector (green), detector readout (red). Right: superposition of 10 rings from incident 5 GeV muons. Units are in mm.

## RICH Detector for the EIC's Forward Region PID

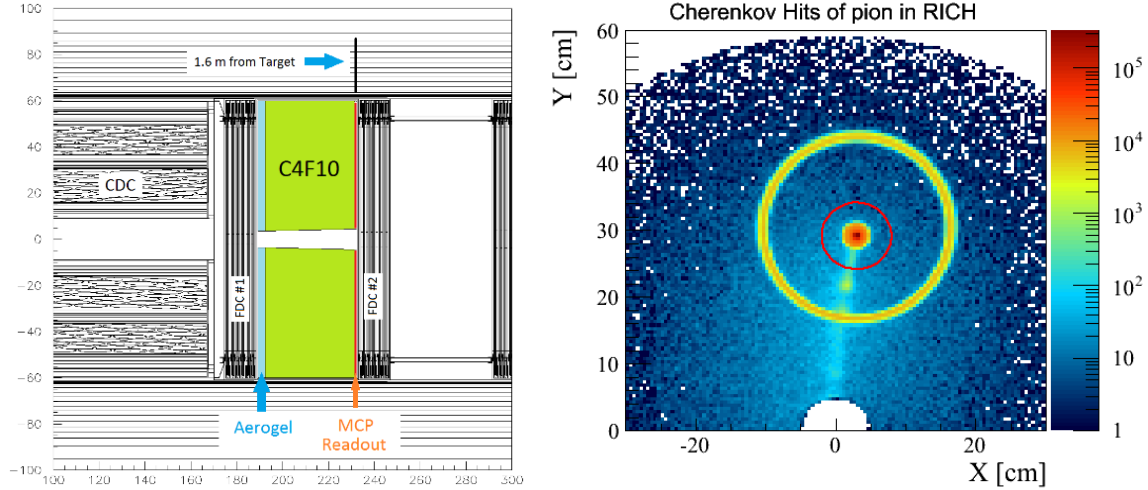


Figure 19. Implementation of a proximity focusing dual-radiator RICH in GlueX's [29] Geant3 framework. Right panel shows a collection of 100k 5-GeV  $\pi^+$  events, both rings from aerogel and blobs from C<sub>4</sub>F<sub>10</sub> are clearly visible. Units are in cm.

### 3.2. Study of MCP-based LAPPD

#### 3.2.1. Year 1 – Characterization

The study of LAPPD will take two steps. During the first year, we will focus on characterizing its basic properties which include:

- Single photon detection efficiency (PDE).
- Background noise level<sup>2</sup>.
- Gain as a function of input pulse rate<sup>3</sup>.
- Time and position resolution.
- Radiation hardness.
- Sensitivity to magnetic field.

Several small (6×6 cm<sup>2</sup>) LAPPD samples will be custom-made by the High Energy Group at Argonne National Lab using the existing LAPPD R&D resources and facilities, which include a glassblowing shop, stations for large area photocathode coating, photocathode characterization and atomic layer deposition, and a vacuum transfer system comprised of several chambers for small LAPPD assembling. The samples will be

<sup>2</sup> Background noise levels have been measured in 33 mm-diameter development MCPs by the LAPPD collaboration (see left panel of Figure 20) and have been shown to be quite low. However this measurement needs to be repeated in a complete detector assembly where noise from the photocathode could significantly increase the background rate.

<sup>3</sup> A preliminary measurement of gain versus rate has been measured for an older 10  $\mu$ m pore MCP alone with an MgO SEE layer and is shown in right panel of Figure 20. This measurement needs to be repeated in a complete detector package.

## RICH Detector for the EIC's Forward Region PID

provided with different readout strips and photocathode. The work at ANL will be led by Dr. Marcel Demarteau and Dr. Robert Wagner. The overall group working on the small format LAPPD production program includes an additional full-time physicist, two postdocs, two engineers and a mechanical engineering assistant.

The tests of LAPPD will be carried out at Jefferson Lab by the Hall-D group and the Detector Group, which both have a lot of experience in various types of photodetectors. Recently, the two groups together studied different types of photomultiplier tubes and silicon photomultipliers (SiPM) for the GlueX experiment [29] in Hall-D including their basic photodetection properties, radiation hardness and tolerance to magnetic field [30][31]. The team was previously awarded of an EIC R&D proposal to study the improved radiation tolerant Silicon photomultipliers [32]. Co-PI Yi Qiang and Dr. Carl Zorn will lead the tests. One thing worth mentioning is that the GlueX collaboration is currently developing a DIRC (detection of internally reflected Cherenkov lights) detector possibly using the retired quartz bars from BaBar [33] for kaon identification in GlueX's forward region. This ongoing activity shares common interests with our proposed project especially in large area photodetector. Therefore a Hall-D postdoc will spend about 45% of time in these tests. A graduate student from Federico Santa Maria Technical University in Chile will also be at JLab during the GlueX's commissioning and participate the LAPPD tests (50%). Additional students and postdocs may be available from other GlueX collaboration universities, such as MIT (contact: Prof. Mike Williams) who is actively participating the development of the GlueX-DIRC detector.

A few sets of readout electronics using the PSEC4 ASICs will be obtained to digitize the LAPPD's signal. Available equipment from Hall-D and the Detector Group, such as a high repetition rate picoseconds blue light pulser, dark boxes, optics, pulse generator, oscilloscopes, complete DAQ system with TDCs and ADCs, high and low voltage power supplies will be used to complete these tests. In particular the picosecond light pulser (PLP-10) that Hall-D purchased from Hamamatsu is an ultrashort pulsed light source with a central wavelength at 405 nm. It has an average 60 ps pulse width and the repetition rate can go up to 100 MHz. It provides an ideal light source to measure the LAPPD's rate capability and timing resolution. The light can also be focused for position resolution measurement.

The radiation hardness test will be coordinated with JLab's Radiation Control Group and both gamma and neutron irradiation sources will be used. Similar studies have been performed earlier on SiPMs [31][32]. The effect of radiation damage on the photodetection efficiency, timing resolution, and gain as well as the noise level will be evaluated. In addition, LANL has neutron and proton irradiation facilities and they will be available for extended tests of radiation hardness. Further, we will use one of Jefferson Lab's spare magnets to test the sensitivity to magnetic field.

## RICH Detector for the EIC's Forward Region PID

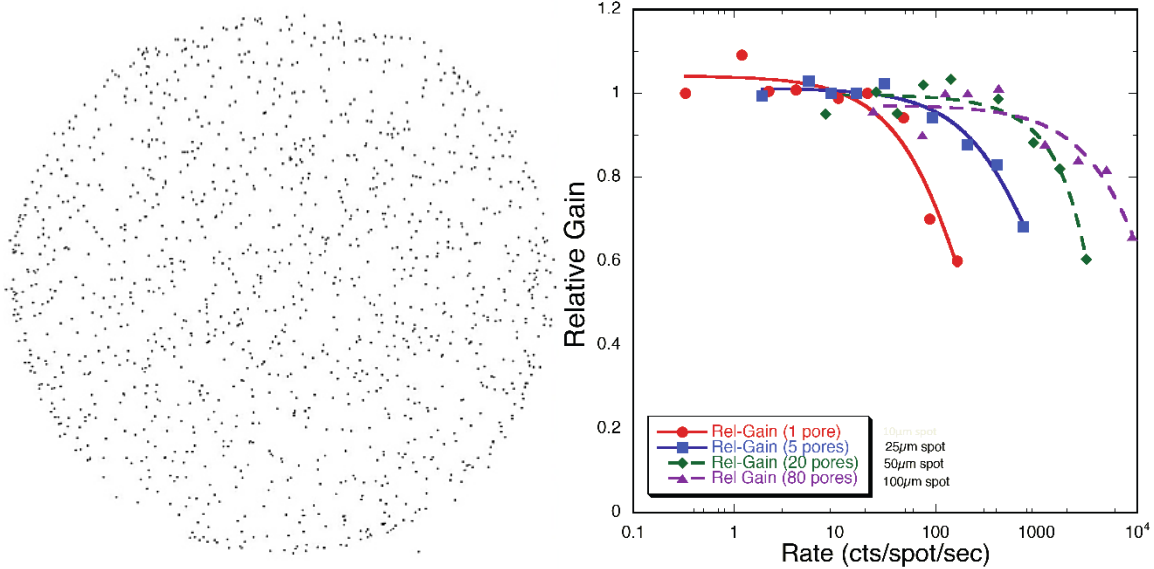


Figure 20. Left: 3000-second background collected on a 33 mm diameter ALD-MCP with 20  $\mu\text{m}$  pores and 1.2 mm thickness. The measured background is 0.84 counts/cm<sup>2</sup>/s at  $7 \times 10^{-6}$  gain and is comparable to cosmic ray induced background. Right: a preliminary measurement of gain as a function of rate for an older 10  $\mu\text{m}$  pre MCP with MgO SEE layer.

### 3.2.2. Year 2 – Improvement

After the initial tests, some of the parameters of the LAPPD may need to be adjusted to better serve the needs of the EIC. A couple of possible items to be addressed are:

- High rate capability.
- Readout ambiguity.

In order to improve the LAPPD's rate, one may think of modifying the chemical composition of the ALD process to improve the discharging speed of the accumulated ions. This will help increase the rate tolerance, possibly at the expense of degraded timing resolution.

The readout ambiguity using LAPPD's existing strip design may become an issue for Cherenkov rings with very small radius, as many photons will hit a small area simultaneously. One possible way to overcome the issue is to narrow the strip width to reduce the multiplicity in a single strip. Because the characteristic impedance of the strip line is a function of both the strip width and glass thickness, such modification would need to be incorporated into an overall package redesign. If the hits are expected to be relatively far apart, a deconvolution algorithm may be implemented in the readout FPGA to further reduce signal overlaps. The Detector Group and the Fast Electronics Group at Jefferson Lab have a lot of related experience in transmission line, fast electronics and FPGA firmware development. Both JLab groups (Sr. Elec. Engineer Jack McKisson, Sr. Elec. Engineer Fernando Barbosa, Dr. Wenzhe Xi and etc.) will work together with Argonne group investigating these options. If ambiguity still imposes an issue after both approaches, we will need to consider the implementation of two-dimensional pixelated

readout options but this will require additional resources beyond this project. It is noted that the LAPPD project is already considering pixilated readout as part of its ongoing R&D program.

### **3.3. Development of Photosensitive GEM Readout**

While GEMs coated with CsI have been used to detect UV photons in previous experiments, the use of a GEM photocathode coating that is sensitive in the wavelength range appropriate for aerogel radiators (~ 300 – 500 nm) has not yet been realized on a large scale. The primary goal of our photosensitive GEM development is to optimize the photocathode deposition parameters and operating gases of GEM to give the highest possible effective quantum efficiency (QE). In addition, appropriate photocathodes developed over the course of this research could be used in conjunction with LAPPD as well. This activity will be led by Co-PI Hubert van Hecke and Dr. Matt Durham from Los Alamos National Lab and Prof. Douglas Fields from University of New Mexico with dedicated efforts of a postdoc (50%) and a graduate student (100%) from UNM.

#### **3.3.1. Year 1 – Initial development**

During year 1, we will first study the two components for photosensitive GEM separately:

- Photocathode on a glass substrate.
- GEM detector with different working gas and readout.

The group of III-V semiconductor materials, such as GaAs, have relatively high quantum efficiencies in the wavelength range of interest to this project, see Figure 17. Development of such photocathodes for high-energy physics experiments has typically been limited by the necessity of using large, expensive, dedicated crystal growth facilities to produce acceptable samples. The University of New Mexico's Center for High Technology Materials (CHTM) is such a facility. The CHTM houses two metal-organic chemical vapor deposition reactors, five molecular beam epitaxial growth reactors, and extensive clean rooms for testing and evaluating semiconductor materials. The CHTM also has the capability to study bialkali photocathodes.

Photocathode development and characterization will proceed as follows. First, candidate materials will be grown at the UNM CHTM, starting with a simple GaAs crystal fixed to glass. The photocathodes will be tested by exposing them to light from LEDs and collecting the resulting current on a charged plate. Comparisons to a reference phototube of known QE will allow the absolute QE of the GaAs samples to be measured. The effects of the electric field at the surface, photocathode thickness, and activation agents (such as CsO) on the current extracted into both vacuum (for the LAPPD application) and gas (for coupling to GEMs) will be studied. The QE in both reflective and transmission modes will be measured. In order to achieve a high total quantum efficiency at the lowest wavelengths of light that will be emitted from the aerogel (~300 nm), gap tuning of the semiconductor materials with the introduction of P into the

## RICH Detector for the EIC's Forward Region PID

material will be studied, in parallel with the photoelectron collection tests. Combinations of glasses that are transparent down to the aerogel cutoff and tuned semiconductors will be measured.

We have already begun a discussion with several of the faculty associated with CHTM and will be receiving our first sample (GaAs) from them to characterize at the Medium Energy Physics lab at UNM. A small vacuum chamber for testing the photocathode's quantum efficiency in vacuum has been identified at UNM.

In the meantime, triple-GEM detector kits, with an x-y strip readout plane and associated electronics, will be purchased from CERN. The performance of GEM for single photon detection will be measured in different gas or mixtures. A list of suitable operating gases will be identified and feed to the development of photocathode. In parallel with these laboratory measurements, readout pattern will be developed in simulation that maximizes the ring resolution with minimum channel count. This readout pattern will then be tested on the bench.

### 3.3.2. Year 2 – Combined Tests

In the second year, we will combine the photocathode developed during the first stage with GEM and LAPPD, and measure the overall performance, particularly the detection efficiency of single photons and the amplitude of signal output. The development of individual components will continue as needed and a few iterations are expected.

### 3.4. Selection of Aerogel Tiles

We will characterize different aerogel samples from Russia, Japan and US to choose the best option for the EIC-RICH. The test will consist of the following items:

- Measurements of transmittance, absorption length and scattering length.
- Measurements of refractive index and chromatic dispersion using the prisms method.
- Refractive index mapping with gradient method.
- High precision mapping of the tiles thickness.

The group will also consider the requirements of a gas system if the tile is hydrophilic when making a final suggestion.

The work will be conducted at Jefferson Lab with assistant from INFN. The two groups have developed skills for the optical characterization of the aerogel radiator for the CLAS12 RICH detector [9] and they have a lot of experience with various types of aerogel detectors. A JLab postdoc (30%) will conduct the tests over the two-year period under the supervision of Co-PI Yi Qiang and Dr. Marco Contalbrigo from INFN who is the key person of the CLAS12 RICH project. Contalbrigo will also be responsible to communicate with all three aerogel manufactures. In addition, the aerogel tests will become very attractive projects for summer SULI (Science Undergraduate Laboratory Internships) students.

## RICH Detector for the EIC's Forward Region PID

To perform measurements of transmittance, absorption length and scattering length a spectrophotometer needs to be purchased for the project. To measure the refractive index and the chromatic dispersion a monochromator coupled to a Xe-UV lamp and monochromatic lasers will fulfill our scope.

In the first year, we will first setup a test stand in one of our clean rooms at JLab, then characterize aerogel samples which are commercially available and try to identify the best manufacture. Then in the second year, we will collaborate with the identified manufacture to optimize the aerogel optical properties for its application in the EIC-RICH.

RICH Detector for the EIC's Forward Region PID

#### 4. Budget

The budget needed to complete the proposed project is listed by activities and institutions in Table 2 and Table 3, respectively.

Table 2. Budget breakdown by activities

Item	Time (FTE)/Cost		Remarks
	Year 1	Year 2	
<b>Simulation</b>			
Equipment	\$4000	\$0	Computers
Staff & Professor	0.3/\$0	0.3/\$0	Free research: 0.1 JLab + 0.1 BNL + 0.1 ODU
Postdoc	0.5/\$45000	0.5/\$45000	0.25 JLab + 0.25 GSU
Student	0.5/\$10000	0.5/\$10000	GSU
Travel	\$6000	\$6000	GSU + BNL
<b>Sub-total</b>	<b>\$65000</b>	<b>\$61000</b>	
<b>LAPPD</b>			
Material	\$20000	\$20000	LAPPD fabrication
Equipment	\$10000	\$5000	PSEC4 readout & test equipment
Staff & Professor	0.8/\$0	1.1/\$0	0.5 – 0.8 JLab (Free research & JLab operation) + 0.3 ANL (ANL base)
Postdoc	0.45/\$25000	0.45/\$25000	0.2 paid by JLab operation
Student	0.5/\$0	0.5/\$0	0.5 UTFSM (paid by UTFSM)
Travel	\$20000	\$20000	JLab + ANL + UTFSM
<b>Sub-total</b>	<b>\$75000</b>	<b>\$70000</b>	
<b>GEM</b>			
Material	\$10000	\$10000	GEM & photocathode material
Equipment	\$10000	\$5000	GEM readout & test equipment
Staff & Professor	0.3/\$9000	0.3/\$9000	0.2 LANL (free research) + 0.1 UNM
Postdoc	0.5/\$40000	0.5/\$40000	UNM
Student	1/\$20000	1/\$20000	UNM
Travel	\$5000	\$5000	LANL
<b>Sub-total</b>	<b>\$94000</b>	<b>\$89000</b>	
<b>Aerogel</b>			
Material	\$10000	\$10000	Aerogel samples
Equipment	\$30000	\$0	Spectrophotometer
Staff & Professor	0.2/\$0	0.2/\$0	Free research: 0.1 JLab + 0.1 INFN
Postdoc	0.3/\$30000	0.3/\$30000	JLab
Student	0.2/\$0	0.2/\$0	Paid by SULI program
Travel	\$5000	\$5000	INFN
<b>Sub-total</b>	<b>\$75000</b>	<b>\$45000</b>	
<b>Grand Total</b>	<b>\$309000</b>	<b>\$265000</b>	

RICH Detector for the EIC's Forward Region PID

Table 3 Budget breakdown by institutions

Item	Time (FTE)/Cost		Remarks
	Year 1	Year 2	
<b>Jefferson Lab</b>			
Material	\$10000	\$10000	Aerogel
Equipment	\$42000	\$5000	Simulation + Aerogel + LAPPD
Staff	0.7/\$0	1.0/\$0	Free research & JLab operation
Postdoc	1/\$80000	1/\$80000	0.2 paid by JLab operation
Travel	\$5000	\$5000	LAPPD
<b>Sub-total</b>	<b>\$137000</b>	<b>\$100000</b>	
<b>Los Alamos National Lab</b>			
Material	\$10000	\$10000	GEM
Equipment	\$10000	\$5000	GEM
Staff	0.2/\$0	0.2/\$0	Free research, GEM
Travel	\$5000	\$5000	GEM
<b>Sub-total</b>	<b>\$25000</b>	<b>\$20000</b>	
<b>Argonne National Lab</b>			
Material	\$20000	\$20000	LAPPD
Staff	0.3/\$0	0.3/\$0	Supported by ANL base funding, LAPPD
Travel	\$5000	\$5000	LAPPD
<b>Sub-total</b>	<b>\$25000</b>	<b>\$25000</b>	
<b>Istituto Nazionale di Fisica Nucleare</b>			
Staff	0.1/\$0	0.1/\$0	Free research, Aerogel
Travel	\$5000	\$5000	Aerogel
<b>Sub-total</b>	<b>\$5000</b>	<b>\$5000</b>	
<b>Brookhaven National Lab</b>			
Staff	0.1/\$0	0.1/\$0	Free research, Simulation
Travel	\$2000	\$2000	Simulation
<b>Sub-total</b>	<b>\$2000</b>	<b>\$2000</b>	
<b>Old Dominion University/JLab</b>			
Equipment	\$2000	\$0	Simulation
Staff	0.1/\$0	0.1/\$0	Free research, Simulation
<b>Sub-total</b>	<b>\$2000</b>	<b>0</b>	
<b>Universidad Tecnica Federico Santa Maria</b>			
Student	0.5/\$0	0.5/\$0	Paid by UTFSM, LAPPD
Travel	\$10000	\$10000	LAPPD
<b>Sub-total</b>	<b>\$10000</b>	<b>\$10000</b>	
<b>The University of New Mexico</b>			
Professor	0.1/\$9000	0.1/\$9000	GEM
Postdoc	0.5/\$40000	0.5/\$40000	GEM
Student	1/\$20000	1/\$20000	GEM
<b>Sub-total</b>	<b>\$69000</b>	<b>\$69000</b>	

RICH Detector for the EIC's Forward Region PID

<b>Georgia State University</b>			
Postdoc	0.25/\$20000	0.25/\$20000	Simulation
Student	0.5/\$10000	0.5/\$10000	Simulation
Travel	\$4000	\$4000	Simulation
<b>Sub-total</b>	<b>\$34000</b>	<b>\$34000</b>	
<b>Grand Total</b>	<b>\$309000</b>	<b>\$265000</b>	

## 5. Further Work

With the completion of this proposed project, we expect to continue the project in a second phase to develop and fabricate a proof-of-principle prototype. With the chosen detector technology including radiators and readout, the collaboration will join the effort on prototyping such a detector. Depending on the conceptual design provided by this project, the approach of future prototyping will vary. Also R&D on some particular detector components may be needed to meet the final requirements.

By the end of the second phase, we will conduct necessary beam tests to demonstrate that the detector's performance will satisfy the EIC's needs on particle identification. As Jefferson Lab will soon have 12 GeV electron beams available in Hall-D, the swept electrons in Hall-D's tagger hall will be an ideal source for these tests. Signal from the tagger hodoscope can be used as a trigger. Various electron rates and energies can be chosen by putting the detector at different locations.

## 6. Summary

An R&D program is proposed to investigate the technology used for a Ring Imaging Cherenkov (RICH) detector for the hadron identification in the forward region of the future Electron-Ion Collider (EIC). Both the dual-radiator RICH option and a modular RICH concept will be investigated and the associated special optics design will be carried out. In particular, a newly developed Large-Area Picoseconds Photo-Detector (LAPPD) using upgraded Micro-Channel Plate (MCP) technology will be carefully evaluated as the readout of the RICH detector. If feasible, the excellent timing resolution provided by this new readout will greatly improve the PID capability of the RICH detector. In parallel, a GEM-based readout option will be investigated as well. At the end, the project will be able to select the best detector technology and provide a conceptual design of the RICH detector for the EIC.

## Bibliography

- [1] RICH Detector for the EIC's Forward Region Particle Identification, PI: Y. Qiang and H. van Hecke, EIC R&D proposal RD 2013-4 (2013), [https://wiki.bnl.gov/conferences/images/2/27/RD2013-4\\_Qiang.pdf](https://wiki.bnl.gov/conferences/images/2/27/RD2013-4_Qiang.pdf)
- [2] *Electron Ion Collider: The Next QCD Frontier*, A. Accardi *et al.*, arXiv:1212.1701 (2012)
- [3] *Concept for and Electron Ion Collider (EIC) detector built around the BaBar solenoid*, PHENIX Collaboration, arXiv:1402.1209 (2014)
- [4] *Use of silica aerogels in Cherenkov counters*, Y. N. Kharzheev, *Phys. of Part. and Nucl.*, **39**, 1 (2008) 107
- [5] *Use of aerogel for imaging Cherenkov counters*, D.E. Fields *et al.*, *Nucl. Instr. and Meth.* **A349** (1994) 431
- [6] *A spot imaging Cherenkov counter*, H. Hecke, *Nucl. Instr. and Meth.* **A343** (1994) 311
- [7] *Budker Institute of Novosibirsk and Boreskov Catalysis Institute of Novosibirsk, Novosibirsk, Russia*
- [8] *Aerogel Cherenkov counters for the KeDR detector*, M.Y. Barnyakov *et al.*, *Nucl. Instr. and Meth.* **A453** (2000) 326
- [9] *The CLAS12 large area RICH detector*, M. Contalbrigo, E. Cisbani, P. Rossi, *Nucl. Instr. and Meth.* **A639** (2011) 302
- [10] Chiba University, Chiba, 263-8522 Japan
- [11] *Aerogel RICH for forward PID at Belle II*, R. Pestotnik *et al.*, *Nucl. Instr. and Meth.* **A732** (2013) 371
- [12] *Silica Aerogel Radiator for Use in the A-RICH System Utilized in the Belle II Experiment*, M. Tabata *et al.*, to be published in *Nucl. Instr. and Meth.* **A**, arXiv:1406.4564 (2014)
- [13] Aspen Aerogels, Inc., Northborough, MA, USA
- [14] *SUVT product details*, A&C Plastics Inc., [http://acplasticsinc.com/techsheets/SUVT\\_ProductDetails.pdf](http://acplasticsinc.com/techsheets/SUVT_ProductDetails.pdf)
- [15] *Proposal for Detector R&D towards an EIC detector*, PI: K. Dehmelt and T. Hemmick, EIC R&D proposal RD-6 (2012), [https://wiki.bnl.gov/conferences/images/9/95/RD2012-16\\_EIC-Tracking\\_proposal\\_April\\_2012.pdf](https://wiki.bnl.gov/conferences/images/9/95/RD2012-16_EIC-Tracking_proposal_April_2012.pdf)
- [16] *The Development of Large-Area Fast Photo-detectors*, The LAPPD Collaboration, Proposal to the Department of Energy's Office of High Energy Physics (2009), [http://psec.uchicago.edu/other/Project\\_description\\_nobudgets.pdf](http://psec.uchicago.edu/other/Project_description_nobudgets.pdf)
- [17] *Development of sub-nanosecond, high gain structures of time-of-flight ring imaging in large area detectors*, the LAPPD collaboration, *Nucl. Instr. and Meth.* **A639** (2011) 148
- [18] *Atomic layer deposited borosilicate glass microchannel plates for large area event counting detectors*, O.W. Siegmund *et al.*, *Nucl. Instr. and Meth.* **A695** (2012) 168

- [19] *RF strip-line anodes for Psec large-area MCP-based photodetectors*, H. Grabas *et al.*, Nucl. Instr. and Meth. **A711** (2013) 124
- [20] *A 15 GSa/s, 1.5 GHz Bandwidth Waveform Digitizing ASIC*, E. Oberia *et al.*, Nucl. Instr. and Meth. **A735** (2014) 452
- [21] *A test-facility for large-area microchannel plate detector assemblies using a pulsed sub-picosecond laser*, B. Adams *et al.*, Rev. of Sci. Instr. **84** (2013) 061301
- [22] *Design, construction, operation and performance of a Hadron Blind Detector for the PHENIX experiment*, W. Anderson *et al.*, Nucl. Instr. and Meth. **A646** (2011) 35
- [23] *Progress in gaseous photomultipliers for the visible spectral range*, Breskin *et al.*, Nucl. Instr. and Meth. **A623** (2010) 318
- [24] *GEant4 Mont-Carlo*, <https://gemc.jlab.org/gemc/Home.html>
- [25] *EIC Detector Software Simulation*, [https://eic.jlab.org/wiki/index.php/EIC\\_Detector\\_Software\\_Simulation](https://eic.jlab.org/wiki/index.php/EIC_Detector_Software_Simulation)
- [26] *A Study of Meson and Baryon Decays to Strange Final States with GlueX in Hall D*, the GlueX Collaboration, Jefferson Lab experiment E12-12-002 (2012), [http://www.jlab.org/exp\\_prog/proposals/12/PR12-12-002.pdf](http://www.jlab.org/exp_prog/proposals/12/PR12-12-002.pdf)
- [27] *Asymmetries in Semi-Inclusive Deep-Inelastic ( $e, e'\pi^\pm$ ) Reactions on a Longitudinally Polarized  $^3\text{He}$  Target at 8.8 and 11 GeV*, Spokespersons: J.-P. Chen, J. Huang, Y. Qiang and W. Yan, Jefferson Lab experiment E12-11-007 (2011), [http://www.jlab.org/exp\\_prog/proposals/11/PR12-11-007.pdf](http://www.jlab.org/exp_prog/proposals/11/PR12-11-007.pdf)
- [28] *PHENIX Planning Documents*, PHENIX collaboration, <http://www.phenix.bnl.gov/plans>
- [29] *Mapping the Spectrum of Light Quark Mesons and Gluonic Excitations with Linearly Polarized Photons*, the GlueX Collaboration, proposal to JLab PAC 30 (2006), [http://www.jlab.org/exp\\_prog/proposals/06/PR12-06-102.pdf](http://www.jlab.org/exp_prog/proposals/06/PR12-06-102.pdf)
- [30] *Silicon photomultiplier characterization for the GlueX barrel calorimeter*, F. Barbosa *et al.*, Nucl. Instr. and Meth. **A695** (2012) 100
- [31] *Radiation Hardness Tests of SiPMs for the JLab Hall D Barrel Calorimeter*, Y. Qiang *et al.*, Nucl. Instr. and Meth. **A698** (2013) 234
- [32] *Proposal to Test Improved Radiation Tolerant Silicon Photomultipliers*, PI: C. Zorn, EIC R&D proposal (2011), [https://wiki.bnl.gov/conferences/images/c/c5/RD-5\\_EIC\\_JLAB\\_SiPM\\_Raddam\\_Proposal-all.pdf](https://wiki.bnl.gov/conferences/images/c/c5/RD-5_EIC_JLAB_SiPM_Raddam_Proposal-all.pdf)
- [33] *The BABAR Detector*, B. Aubert *et al.* (BABAR Collaboration), Nucl. Instr. and Meth. **A479** (2002) 1